Metallosupramolecules bearing Pendant Redox-active Domains: Synthesis and Co-ordination Behaviour of the Metallocene-functionalized Helicand 4′,4‴″-Di(ferrocenyl)-2,2′:6′,2″:6″,2‴:6‴,2⁗:6⁗,2⁗′-sexipyridine†

Edwin C. Constable,*[a] Andrew J. Edwards,[b] Ramón Martínez-Máñez*[b,c] and Paul R. Raithby[b]

[a] *Institut für Anorganische Chemie, Spitalstrasse 51, CH-4056, Basel, Switzerland*

[b] *Cambridge Centre for Molecular Recognition and Centre for Chemical Crystallography, University Chemical Laboratory, University of Cambridge, Lensfield Road, Cambridge CB2 1EW, UK*

[c] *Departamento de Química, Universidad Politécnica de Valencia, Camino de Vera, s/n, Valencia, Spain*

The novel ferrocene-functionalized helicand 4′,4⁗′-di(ferrocenyl)-2,2′:6′,2″:6″,2‴:6‴,2⁗:6⁗,2⁗′-sexipyridine (dfspy) has been obtained from the reaction of 6,6′-di(1-pyridinioacetyl)-2,2′-bipyridine diiodide and 2-[3-(ferrocenyl)-1-oxoprop-2-enyl]pyridine. However, a related route involving the condensation of 6,6′-di[3-(ferrocenyl)-1-oxoprop-2-enyl]-2,2′-bipyridine **I** with *N*-[2-oxo-2-(2-pyridyl)ethyl]pyridinium iodide does not give the desired sexipyridine derivative. In an attempt to understand these reactivity patterns the crystal structure of **I** has been determined by single-crystal X-ray methods: monoclinic, space group $P2_1/n$, $a = 5.8780(10)$, $b = 12.622(3)$, $c = 24.860(5)$ Å, $\beta = 93.33(3)°$, $Z = 4$. A nickel(0) template procedure for the synthesis of dfspy from 6-bromo-4′-ferrocenyl-2,2′:6′,2″-terpyridine (bfterpy) has also been investigated. The co-ordination behaviour of the new redox-active compounds bfterpy and dfspy has been studied. The interaction of bfterpy with metal salts gives the mononuclear complexes $[M(bfterpy)_2][PF_6]_2$ (M = Fe, Co, Ni or Zn). In contrast, with dfspy the double-helical complexes $[M_2(dfspy)_2][PF_6]_4$ (M = Fe, Co, Ni or Zn) are formed.

There is considerable interest in the design of new ligands the topology of which can be controlled by interaction with metal ions through self-assembly (metallosupramolecular chemistry). In particular, the oligopyridines have proved to be versatile ligands which can give rise to different geometries upon co-ordination to transition-metal ions, dependent upon the number and distribution of the donor sites and the co-ordination requirements of the metal.[1] We have recently developed a multiphasic approach to metallosupramolecular chemistry, and have been concerned with the design and synthesis of species in which a number of discrete functional regions may be identified.[2] At its simplest, such an approach results in the need for ligands with spatially separated metal binding and functionalized domains. We have recently introduced redox-active sites onto the periphery of oligopyridine ligands, as a prelude further to exploring the self-assembly processes with transition-metal ions and the interactions between the peripheral redox centres and metal ions co-ordinated to the oligopyridine domains.

One class of redox-active substituents is the metallocenes, and a variety of ferrocene-containing systems[3-12] including the ferrocene-functionalized oligopyridine ligands 4′-ferrocenyl-2,2′:6′,2″-terpyridine,[7,8] 4,4‴-di(ferrocenyl)-2,2′:6′,2″:6″,2‴:6‴,2⁗-quinquepyridine,[9] 1,1′-(2,2′:6′,2″-terpyridin-4′-yl)ferrocene[10,11] and a novel ferrocenophane.[11,12] We now describe the new helicand 4′,4⁗′-di(ferrocenyl)-2,2′:6′,2″:6″,2‴:6‴,2⁗:6⁗,2⁗′-sexipyridine and its interaction with transition-metal ions.

Experimental

Infrared spectra were recorded on a Philips PU9624 Fourier-transform spectrophotometer, with the samples as compressed KBr discs, electronic spectra on a PU8730 spectrophotometer, ^{1}H NMR spectra on a Bruker WM-250 spectrometer and fast atom bombardment (FAB) spectra on a Kratos MS-50 spectrometer. Electrochemical experiments were performed using an Autolab PGSTAT20 instrument. Differential pulse voltammetry was performed with a pulse amplitude of 25 mV, step rate of 10 mV s^{-1} and a 'drop time' of 0.5 s. A conventional three-electrode configuration was used with platinum-bead working and auxiliary electrodes and a Ag–Ag$^+$ electrode as reference. The solvent was purified acetonitrile or dichloromethane–acetonitrile and the supporting electrolyte was 0.1 mol dm^{-3} $[NBu_4][BF_4]$ recrystallized twice from ethanol–water. Ferrocene was added at the end of each experiment as an internal standard. *N*-[2-Oxo-2-(2-pyridyl)ethyl]pyridinium iodide,[13] 6,6′-di(1-pyridinioacetyl)-2,2′-bipyridine diiodide,[14] 2-[3-(ferrocenyl)-1-oxoprop-2-enyl]pyridine,[8] 2-acetyl-6-bromopyridine[15] and 6,6′-diacetyl-2,2′-bipyridine[15] were prepared according to published procedures.

Preparations.—*6,6′-Di*[3-(*ferrocenyl*)-1-*oxoprop*-2-*enyl*]-2,2′-*bipyridine* **I**. 6,6′-Diacetyl-2,2′-bipyridine (0.240 g, 1 mmol) and ferrocenecarbaldehyde (1.070 g, 5 mmol) were heated to reflux in a mixture of propan-2-ol (6 cm^3) and diethylamine (1 cm^3) for 3 h. After cooling the reaction mixture to room temperature, the purple-red solid obtained was filtered off, washed with small amounts of propan-2-ol and dried *in vacuo* to give compound **I** (0.427 g, 75%) (Found: C, 66.45; H, 4.40; N, 4.35. Calc. for $C_{36}H_{28}Fe_2N_2O_2{\cdot}H_2O$: C, 66.45; H, 4.60; N, 4.30%). IR (KBr): 1663s, 1593s, 1385s, 1348w, 1318m, 1224w, 1175w, 1077w, 1027m, 973m, 812m, 749w, 651w, 495w and 483w cm^{-1}. ^{1}H NMR ($CDCl_3$): δ 4.21 (s, 10 H, C_5H_5), 4.54 (t, 4 H, C_5H_4), 4.71 (t, 4 H, C_5H_4), 7.94 (d, 2 H, CH), 8.02 (d, 2 H, CH), 8.08 (t, 2 H, H^4), 8.26 (dd, 2 H, H^3) and 8.77 (dd, 2 H, H^5). Mass spectrum (FAB): *m*/*z* 633 (*P* + 1).

† *Supplementary data available:* see Instructions for Authors, *J. Chem. Soc., Dalton Trans.*, 1995, Issue 1, pp. xxv–xxx.

4′,4‴′-Di(ferrocenyl)-2,2′:6′,2″:6″,2‴:6‴,2⁗:6⁗,2⁗′-sexipyridine (*dfspy*). 6,6′-Di(1-pyridinioacetyl)-2,2′-bipyridine diiodide (1.000 g, 1.53 mmol), 2-[3-(ferrocenyl)-1-oxoprop-2-enyl]pyridine (0.971 g, 3.06 mmol) and ammonium acetate (4 g) were added to ethanol (30 cm^3) and the mixture heated to reflux for 16 h. After cooling the reaction mixture, the crude solid product was filtered off and washed well with ethanol and methanol. This solid was then added to toluene (150 cm^3) and the solution boiled in the presence of activated charcoal for 10 min. The mixture was then filtered through Celite and the yellow filtrate concentrated to 30 cm^3 volume and cooled. An orange-yellow solid was obtained which was filtered off and dried *in vacuo* to give dfspy (0.250 g, 20%) (Found: C, 72.20; H, 4.30; N, 10.15. Calc. for $C_{50}H_{36}Fe_2N_6$: C, 72.15; H, 4.35; N, 10.10%). IR (KBr): 1601m, 1585s, 1567s, 1547s, 1474w, 1406s, 1385s, 1274w, 1107w, 1022w, 990w, 890w, 810m, 795m, 741w, 659w and 500m cm^{-1}. ^1H NMR ($CDCl_3$): δ 4.15 (s, 10 H, C_5H_5), 4.51 (t, 4 H, C_5H_4), 5.04 (t, 4 H, C_5H_4), 7.37 (ddd, 2 H, $H^{5,5''''}$), 7.90 (dt, 2 H, $H^{4,4''''}$), 8.12 (t, 2 H, $H^{4'',4'''}$), 8.56 (d, 2 H, $H^{3'/5',3''''/5''''}$) and 8.70–8.82 (m, 10 H, $H^{5''/3'',5''''/3''''3,3''''',6,6''''',3'',3''',5'',5'''}$). Mass spectrum (FAB): *m/z* 833 (*P* + 1).

6-Bromo-2-[3-(ferrocenyl)-1-oxoprop-2-enyl]pyridine **II**. 2-Acetyl-6-bromopyridine (0.800 g, 4 mmol) and ferrocenecarbaldehyde (0.856 g, 4 mmol) were dissolved in ethanol (35 cm^3), and after 2 min aqueous sodium hydroxide solution (6 cm^3, 2 mol dm^{-3}) was added and the resultant mixture stirred for 30 min. After this period water (10 cm^3) was added and the purple-red precipitate was filtered off and washed with ethanol–water (1:3 v/v) and dried *in vacuo* to give compound **II** (1.425 g, 90%) (Found: C, 54.10; H, 3.55; N, 3.45. Calc. for $C_{18}H_{14}BrFeNO$: C, 54.55; H, 3.55; N, 3.55%). IR (KBr): 1661m, 1585s, 1563m, 1548m, 1394w, 1360m, 1312w, 1116m, 1105w, 1032m, 985m, 829w, 814w, 755w, 621w and 496w cm^{-1}. ^1H NMR ($CDCl_3$): δ 4.18 (s, 5 H, C_5H_5), 4.52 (t, 2 H, C_5H_4), 4.68 (t, 2 H, C_5H_4), 7.64 (dd, 1 H, H^5), 7.71 (t, 1 H, H^4), 7.72 (d, 1 H, CH), 7.90 (d, 1 H, CH) and 8.13 (dd, 1 H, H^3). Mass spectrum (FAB): *m/z* 395/397 (*P*).

6-Bromo-4′-ferrocenyl-2,2′:6′,2″-terpyridine (*bfterpy*). Compound **II** (1.000 g, 2.53 mmol) and *N*-[2-oxo-2-(2-pyridyl)-ethyl]pyridinium iodide (0.823 g, 2.53 mmol) were heated to reflux in ethanol (40 cm^3) in the presence of ammonium acetate (4 g) for 2 h. The reaction mixture was filtered hot, and the yellow-orange solid product was washed with ethanol, methanol and water and dried *in vacuo* to give bfterpy (0.900 g, 72%) (Found: C, 60.70; H, 3.60; N, 8.25. Calc. for $C_{25}H_{18}BrFeN_3$: C, 60.50; H, 3.65; N, 8.45%). IR (KBr): 1601m, 1587s, 1568m, 1546s, 1478m, 1406s, 1384s, 1124m, 1107w, 1022w, 983w, 805m, 746m and 498m cm^{-1}. ^1H NMR ($CDCl_3$): δ 4.09 (s, 5 H, C_5H_5), 4.47 (t, 2 H, C_5H_4), 5.00 (t, 2 H, C_5H_4), 7.35 (ddd, 1 H, $H^{5''}$), 7.51 (d, 1 H, H^5), 7.70 (t, 1 H, H^4), 7.86 (dt, 1 H, $H^{4''}$), 8.45 (d, 1 H, $H^{3'/5'}$), 8.52 (d, 1 H, $H^{5'/3'}$), 8.60 (d, 2 H, $H^{3,3''}$) and 8.73 (dd, 1 H, $H^{6''}$). Mass spectrum (FAB): *m/z* 495/497 (*P*).

$[M(bfterpy)_2][PF_6]_2$ (M = Fe, Co, Ni *or* Zn). A solution of the appropriate metal acetate (0.25 mmol) or $FeCl_2{\cdot}4H_2O$ (0.25 mmol) in ethanol–water (3:1 v/v, 6 cm^3) was added to a stirred solution of bfterpy (0.250 g, 0.5 mmol) in dichloromethane–ethanol (3:1 v/v, 40 cm^3). After 10 min the reaction mixture was treated with an excess of aqueous $[NH_4][PF_6]$ and concentrated to give a solid. This was filtered off and recrystallized by dissolving in acetone, adding methanol and concentrating *in vacuo* until crystallization commenced. After cooling, the solid was filtered off and dried *in vacuo*.

The iron complex was obtained as a deep blue solid, $[Fe(bfterpy)_2][PF_6]_2$ (0.217 g, 65%) (Found: C, 43.70; H, 2.90; N, 6.15. Calc. for $C_{50}H_{36}Br_2F_{12}Fe_3N_6P_2{\cdot}2H_2O$: C, 43.65; H, 2.90; N, 6.10%). IR (KBr disc): 1609m, 1557m, 1498w, 1460m, 1432w, 1413w, 1385m, 1252w, 1185w, 1107w, 1021w, 842s, 741w, 714w and 558m cm^{-1}. ^1H NMR (CD_3CN): δ 3.2 (br), 3.7 (br), 4.1 (br), 15.1 (br), 17.8 (br), 44.4 (br), 45.1 (br), 48.1 (br), 49.1 (br), 58.2 (br) and 67.5 (br). Mass spectrum (FAB): *m/z* 1338 $\{[Fe(bfterpy)_2][PF_6]_2\}$, 1193 $\{[Fe(bfterpy)_2][PF_6]\}$ and 1048 $\{[Fe(bfterpy)_2]\}$.

The cobalt complex was obtained as a red solid, $[Co(bfterpy)_2][PF_6]_2$ (0.200 g, 60%) (Found: C, 44.35; H, 2.65; N, 6.25. Calc. for $C_{50}H_{36}Br_2CoF_{12}Fe_2N_6P_2$: C, 44.75; H, 2.70; N, 6.25%). IR (KBr): 1608m, 1558m, 1497w, 1460m, 1432w, 1413w, 1385m, 1185w, 1135w, 1107w, 1057w, 840s, 740w, 714w and 558m cm^{-1}. ^1H NMR (CD_3CN): δ −11.8 (br), 11.7 (br), 11.9 (br), 17.4 (br), 20.4 (br), 20.6 (br), 35.6 (br), 49.4 (br), 54.2 (br), 78.8 (br), 105.5 (br) and 137.6 (br). Mass spectrum (FAB): *m/z* 1342 $\{[Co(bfterpy)_2][PF_6]_2\}$, 1196 $\{[Co(bfterpy)_2][PF_6]\}$ and 1052 $\{[Co(bfterpy)_2]\}$.

The nickel complex was obtained as a red solid $[Ni(bfterpy)_2][PF_6]_2$ (0.211 g, 63%) (Found: C, 45.30; H, 2.85; N, 6.20. Calc. for $C_{50}H_{36}Br_2F_{12}Fe_2N_6NiP_2$: C, 44.75; H, 2.70; N, 6.25%). IR (KBr): 1609s, 1558m, 1496w, 1462m, 1433m, 1413m, 1385m, 1255w, 1186w, 1135w, 1107w, 1037m, 840s, 741w, 716w and 558m cm^{-1}. ^1H NMR (CD_3CN): δ 4.9 (br), 5.2 (br), 7.4 (br), 8.3 (br), 14.1 (br), 45.2 (br), 47.4 (br), 54.2 (br), 66.1 (br) and 77.1 (br). Mass spectrum (FAB): *m/z* 1341 $\{[Ni(bfterpy)_2][PF_6]_2\}$, 1195 $\{[Ni(bfterpy)_2][PF_6]\}$ and 1051 $\{[Ni(bfterpy)_2]\}$.

The zinc complex was obtained as a red solid, $[Zn(bfterpy)_2][PF_6]_2$ (0.218 g, 65%) (Found: C, 44.95; H, 2.75; N, 6.15. Calc. for $C_{50}H_{36}Br_2F_{12}Fe_2N_6P_2Zn$: C, 44.55; H, 2.65; N, 6.25%). IR (KBr): 1693m, 1609s, 1557m, 1498w, 1459m, 1431m, 1384m, 1245w, 1185w, 1136w, 1106w, 1023w, 844s, 713w and 557m cm^{-1}. ^1H NMR (CD_3CN): δ 4.26 (s, 10 H, C_5H_5), 4.84 (t, 4 H, C_5H_4), 5.38 (t, 4 H, C_5H_4), 7.40 (ddd, 2 H, $H^{5''}$), 7.58 (d, 2 H, $H^{6''}$), 7.74 (d, 2 H, H^5), 8.11–8.16 (m, 4 H, $H^{4,4''}$), 8.63 (s, 2 H, $H^{3'/5'}$), 8.66 (d, 2 H, $H^{3''}$), 8.67 (s, 2 H, $H^{5'/3'}$) and 8.82 (d, 2 H, H^3). Mass spectrum (FAB): *m/z* 1348 $\{[Zn(bfterpy)_2][PF_6]_2\}$, 1203 $\{[Zn(bfterpy)_2][PF_6]\}$ and 1059 $\{[Zn(bfterpy)_2]\}$.

$[M_2(dfspy)_2][PF_6]_4$ (M = Fe, Co, Ni *or* Zn). A mixture of dfspy (0.200 g, 0.24 mmol) and the appropriate metal acetate or $FeCl_2{\cdot}4H_2O$ (0.24 mmol) was heated to reflux in methanol (40 cm^3) for 1.5 h. After this period the reaction mixture was cooled and filtered through Celite. In the case of the cobalt and zinc complexes, thin-layer chromatography (silica, 30:2:1 MeCN, aqueous saturated KNO_3 solution and water) of the filtrate revealed a major violet band whilst with iron or nickel two main bands (red and violet) were obtained. In each case the reaction mixture was evaporated to dryness *in vacuo* and the crude solid dissolved in acetonitrile and chromatographed on silica using the same mobile phase as for the TLC analysis. The violet fractions were treated with aqueous $[NH_4][PF_6]$ and the solutions concentrated until the appearance of a precipitate which was then filtered off, washed well with water and dried *in vacuo*.

The iron complex was obtained as a blue-violet solid, $[Fe_2(dfspy)_2][PF_6]_4$ (0.057 g, 20%) (Found: C, 49.85; H, 3.10; N, 7.20. Calc. for $C_{100}H_{72}F_{24}Fe_6N_{12}P_4$: C, 50.95; H, 3.05, N, 7.15%). IR (KBr): 1605s, 1567m, 1542w, 1495w, 1464m, 1436w, 1385m, 1355m, 1251w, 1107w, 1021m, 842s, 739w, 681w, 558m and 507w cm^{-1}. ^1H NMR (CD_3CN): δ 3.2 (br), 4.2 (br), 4.4 (br), 4.8 (br), 5.3 (br), 9.1 (br), 17.6 (br), 39.2 (br), 56.0 (br), 57.1 (br), 72.1 (br), 83.4 (br) and 175.8 (br). Mass spectrum (FAB): *m/z* 2211 $\{[Fe_2(dfspy)_2][PF_6]_3\}$, 2066 $\{[Fe_2(dfspy)_2][PF_6]_2\}$ and 888 $\{[Fe(dfspy)]\}$.

The cobalt complex was obtained as a red-violet solid, $[Co_2(dfspy)_2][PF_6]_4$ (0.119 g, 42%) (Found: C, 49.70; H, 3.10; N, 7.15. Calc. for $C_{100}H_{72}Co_2F_{24}Fe_4N_{12}P_4$: C, 50.85; H, 3.05; N, 7.10%). IR (KBr): 1607s, 1569m, 1545w, 1496w, 1465m, 1438w, 1420w, 1385m, 1358w, 1252w, 1169w, 1108w, 1023m, 844s, 791m, 558m and 510w cm^{-1}. ^1H NMR (CD_3CN): δ −40.5 (br), −19.2 (br), 13.8 (br), 14.7 (br), 15.7 (br), 17.4 (br), 18.1 (br), 33.6 (br), 40.5 (br), 45.2 (br), 72.4 (br), 132.5 (br) and 154.4 (br). Mass spectrum (FAB): *m/z* 2218 $\{[Co_2(dfspy)_2][PF_6]_3\}$, 2073 $\{[Co_2(dfspy)_2][PF_6]_2\}$, 1928 $\{[Co_2(dfspy)_2][PF_6]\}$ and 890 $\{[Co(dfspy)]\}$.

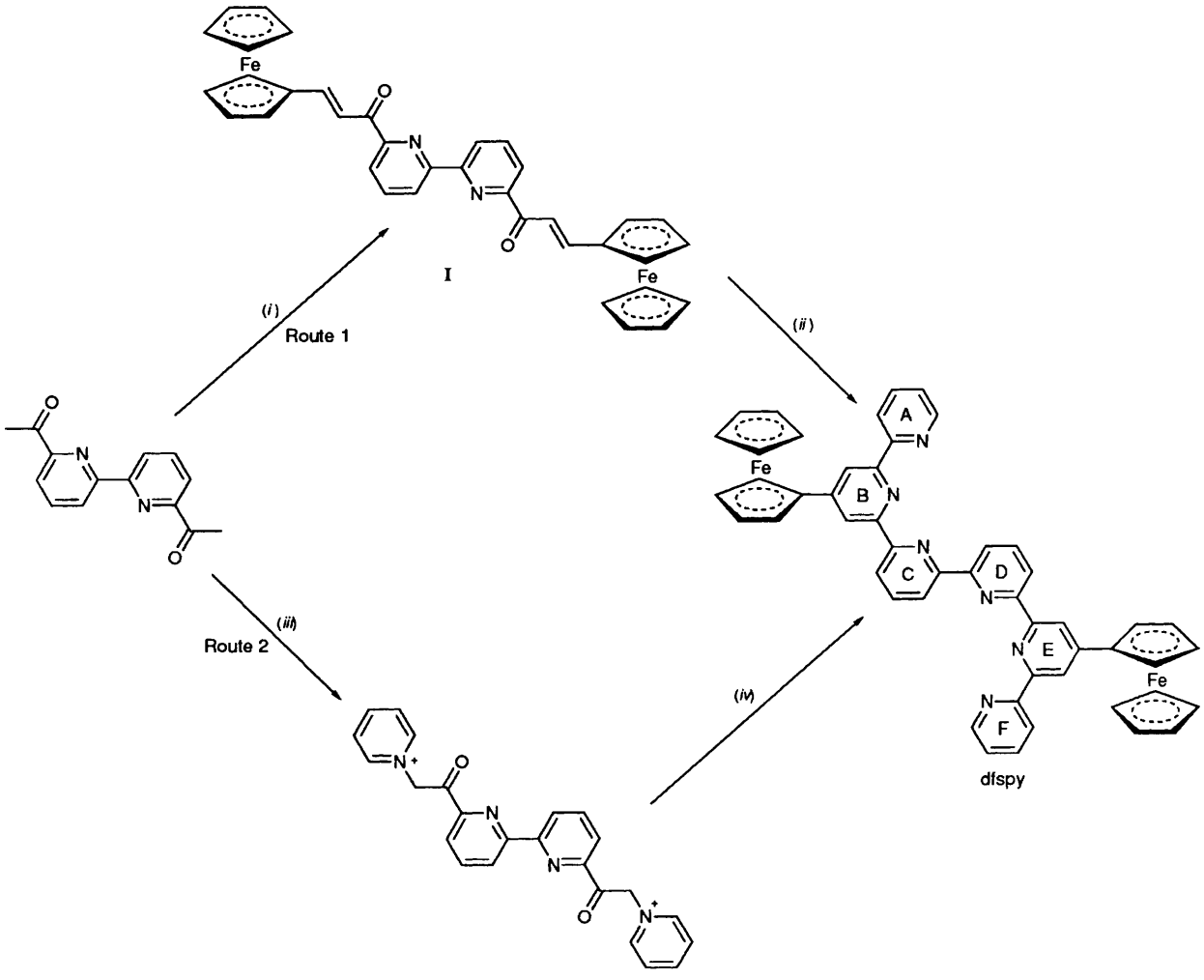

Scheme 1 (*i*) Ferrocenecarbaldehyde; (*ii*) [2-oxo-2-(2-pyridyl)ethyl]pyridinium iodide, $[NH_4][O_2CMe]$; (*iii*) pyridine, I_2; (*iv*) 2-[3-(ferrocenyl)-1-oxoprop-2-enyl]pyridine, $[NH_4][O_2CMe]$

The nickel complex was obtained as a red-violet solid, $[Ni_2(dfspy)_2][PF_6]_4$ (0.053 g, 19%) (Found: C, 49.95; H, 3.05; N, 7.10. Calc. for $C_{100}H_{72}F_{24}Fe_4N_{12}Ni_2P_4$: C, 50.85; H, 3.05; N, 7.10%). Infrared spectrum (KBr disc): 1608s, 1569m, 1547w, 1496w, 1467m, 1438w, 1420w, 1385m, 1354m, 1251w, 1107w, 1031m, 844s, 791m, 740w, 558m and 510w cm^{-1}. ^1H NMR (CD_3CN): δ 3.5 (br), 4.7 (br), 5.3 (br), 7.3 (br), 10.4 (br), 13.8 (br), 41.7 (br), 45.3 (br), 61.5 (br), 64.0 (br), 66.9 (br) and 75.1 (br). Mass spectrum (FAB): *m/z* 2217 $\{[Ni_2(dfspy)_2][PF_6]_3\}$, 2072 $\{[Ni_2(dfspy)_2][PF_6]_2\}$ and 890 $\{[Ni(dfspy)]\}$.

The zinc complex was obtained as a blue-violet solid, $[Zn_2(dfspy)_2][PF_6]_4$ (0.077 g, 27%) (Found: C, 49.70; H, 3.00; N, 7.10. Calc. for $C_{100}H_{72}F_{24}Fe_4N_{12}P_4Zn_2$: C, 50.55; H, 3.05; N, 7.10%). IR (KBr): 1607s, 1570m, 1546m, 1497w, 1465m, 1437w, 1413w, 1385m, 1355w, 1254w, 1108w, 1024m, 842s, 739w, 558m and 507w cm^{-1}. ^1H NMR (CD_3CN): δ 4.31 (br, 20 H, C_5H_5), 4.95 (br, 4 H, C_5H_4), 4.98 (br, 4 H, C_5H_4), 5.43 (br, 4 H, C_5H_4), 5.48 (br, 4 H, C_5H_4), 6.89 (d, 4 H, $H^{5'',5'''}$), 7.02 (d, 4 H, $H^{6,6''''}$), 7.24 (t, 4 H, $H^{5,5''''}$), 7.72 (t, 4 H, $H^{4'',4'''}$), 8.04 (t, 4 H, $H^{4,4''''}$), 8.44–8.54 (m, 16 H, $H^{3,3'''',3',3'''',5',5'''',3'',3'''}$). Mass spectrum (FAB): *m/z* 2230 $\{[Zn_2(dfspy)_2][PF_6]_3\}$, 2085 $\{[Zn_2(dfspy)_2][PF_6]_2\}$ and 896 $\{[Zn(dfspy)]\}$.

Structure Determination of Compound **I**.—*Crystal data.* $C_{19}H_{15}Cl_3FeNO$, M = 435.52, monoclinic, space group $P2_1/n$, a = 5.8780(10), b = 12.622(3), c = 24.860(5) Å, β = 93.33(3)°, U = 1841.3(7) $Å^3$, Z = 4, $F(000)$ = 884, D_c = 1.571 g cm^{-3}, λ(Mo-Kα) = 0.710 69 Å, T = 153(2) K, μ(Mo-Kα) = 12.6 cm^{-1}.

Data collection and refinement. Data were collected on a Siemens Stoe AED four-circle diffractometer using a crystal of dimensions 0.21 × 0.19 × 0.18 mm by the 2θ–ω method ($7.0 \leqslant 2\theta \leqslant 45.0°$). Of 2671 reflections collected, 2399 were unique (R_{int} = 0.026). The structure was solved by direct methods (SHELXTL PLUS[16]) and refined by full-matrix least-squares analysis on F^2 (SHELXL 93[17]) to $R1$ 0.052 [$F > 4\sigma(F)$, for 1945 reflections] and $R2$ 0.205 (all data) where $R1 = \Sigma||F_o| - |F_c||/\Sigma|F_o|$, $R2 = [\Sigma w(F_o^2 - F_c^2)^2/\Sigma wF_o^4]^{\frac{1}{2}}$, $w = 1/[\sigma^2(F_o^2) + (xP)^2 + yP]$ and $P = (F_o^2 + 2F_c^2)/3$. Largest peak and hole in the final difference map +0.92, −1.56 e $Å^{-3}$. Final atomic coordinates for non-hydrogen atoms and relevant bond lengths and angles are presented in Tables 1 and 2.

Additional material available from the Cambridge Crystallographic Data Centre comprises H-atom coordinates, thermal parameters and remaining bond lengths and angles.

Results and Discussion

A number of possible routes to ferrocenyl-substituted spy ligands may be envisaged. As we planned to introduce the ferrocenyl group in the form of ferrocenecarbaldehyde, we could not adopt any of the methodology developed by Potts *et al.*[18] Two potential routes for the synthesis of 4′,4‴-di(ferrocenyl)-substituted spy ligands are depicted in Scheme 1. The approaches delineated are based upon the use of 6,6′-diacetyl-2,2′-bipyridine to generate rings C and D and 2-acetylpyridine as the origin of the A and F rings. The two

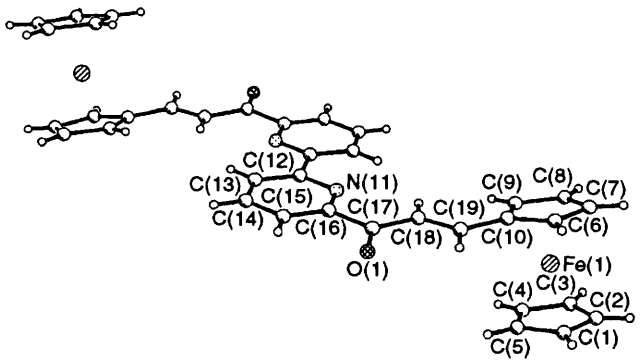

Fig. 1 Crystal structure of compound **I** showing the atomic numbering scheme adopted

remaining pyridine rings, B and E, are generated by a Krohnke-type pyridine synthesis.[13]

In route 1, 6,6′-diacetyl-2,2′-bipyridine is treated with ferrocenecarbaldehyde to give 6,6′-di[3-(ferrocenyl)-1-oxoprop-2-enyl]-2,2′-bipyridine **I**. This latter compound is then converted into dfspy by reaction with *N*-[2-oxo-2-(2-pyridyl)ethyl]pyridinium iodide. In route 2, the pyridinium salt 6,6′-di(1-pyridinioacetyl)-2,2′-bipyridine diiodide is prepared by the reaction of 6,6′-diacetyl-2,2′-bipyridine with iodine in pyridine, whilst the enone 2-[3-(ferrocenyl)-1-oxoprop-2-enyl]pyridine is obtained from 2-acetyl-pyridine and ferrocenecarbaldehyde. The basis of the Krohnke method[13] is the use of a pyridinium salt as a masked enone (or ylide) to generate 1,5-dicarbonyl intermediates which are cyclized *in situ* by reaction with ammonium acetate. The applicability of routes 1 and 2 depends then on the relative reactivity of both the pyridinium salt and the enone derivative. In the past we have used both of these routes for the preparation of spy ligands; route 2 provided the basis for the preparation of the parent spy ligand[14] and more recently we have used route 1 for the preparation of the solubilized ligand 4′,4‴-di(4-*tert*-butylphenyl)-2,2′:6′,2″:6″,2‴:6‴,2⁗:6⁗,2⁗′-sexipyridine (dbpspy).[19] With simple aromatic aldehydes, both routes give acceptable yields of the desired 4′,4‴-diaryl-substituted spy ligands.[20]

Initially, we decided to adopt route 1. The reaction of 6,6′-diacetyl-2,2′-bipyridine with ferrocenecarbaldehyde gave compound **I** as a purple-red solid showing a characteristic strong ν(C=O) stretching vibration at 1663 cm^{-1} in its infrared spectrum, typical of a 2-pyridyl enone.[19] The ^1H NMR spectrum of a $CDCl_3$ solution of **I** was fully in accord with the proposed structure, as were the mass spectrum (FAB, m/z = 633) and elemental analysis. Compound **I** behaves as a typical ferrocene derivative, and is electroactive with a single reversible two-electron Fe^{II}–Fe^{III} process at +0.11 V (CH_2Cl_2 as solvent, potential quoted *versus* ferrocene, see Table 3) along with two reduction processes at −1.60 and −2.09 V.

The reaction of compound **I** with *N*-[2-oxo-2-(2-pyridyl)-ethyl]pyridinium iodide in the presence of an excess of ammonium acetate in ethanol gave, upon cooling after 24 h at reflux, a yellow solid. This was filtered off and shown to be primarily the starting material **I**. Repeating the reaction using ethanol, mixtures of ethanol and acetic acid or pure acetic acid as solvent did not yield any of the desired dfspy. This lack of reactivity found for **I** in its reaction with the Krohnke salt contrasts markedly with the behaviour of related ferrocene-fuctionalized enones such as 2,6-di[3-(ferrocenyl)-1-oxoprop-2-enyl]pyridine, 2-[3-(ferrocenyl)-1-oxoprop-2-enyl]pyridine and 1,1′-di[3-oxo-3-(2-pyridyl)prop-2-enyl]ferrocene which we have found to be suitable starting materials for the synthesis of ferrocene-substituted quinquepyridine[9] and terpyridine[7,8,10–12] derivatives. We found the lack of reactivity of **I** sufficiently surprising that we determined its single-crystal structure in order to ascertain whether there were any structural peculiarities which might explain its inertness.

Table 1 Atomic coordinates ($\times 10^4$) for all non-hydrogen atoms in compound **I**

Atom	x	y	z
Fe(1)	0.4442(1)	0.2092(1)	0.2120(1)
O(1)	0.1662(8)	0.2793(4)	−0.0100(2)
C(1)	0.5070(13)	0.3665(5)	0.2269(3)
C(2)	0.5238(12)	0.3103(6)	0.2752(3)
C(3)	0.3141(12)	0.2600(6)	0.2822(3)
C(4)	0.1644(11)	0.2881(5)	0.2371(3)
C(5)	0.2839(13)	0.3524(5)	0.2032(3)
C(6)	0.6735(11)	0.1564(5)	0.1588(2)
C(7)	0.6996(11)	0.0974(5)	0.273(3)
C(8)	0.4878(11)	0.0475(5)	0.2168(3)
C(9)	0.3272(11)	0.0735(5)	0.1734(2)
C(10)	0.4416(10)	0.1420(5)	0.1369(2)
N(11)	−0.2512(8)	0.0841(4)	0.0093(2)
C(12)	−0.4426(11)	0.0426(5)	−0.0150(2)
C(13)	−0.5323(11)	0.0755(5)	−0.0654(2)
C(14)	−0.4156(12)	0.1555(5)	−0.0916(3)
C(15)	−0.2179(12)	0.1978(5)	−0.0677(3)
C(16)	−0.1433(10)	0.1600(5)	−0.0171(2)
C(17)	0.0674(11)	0.2056(5)	0.0112(3)
C(18)	0.1467(11)	0.1579(5)	0.0625(2)
C(19)	0.3427(11)	0.1888(5)	0.0877(2)
C(20)	−0.6870(12)	0.4640(5)	−0.0793(3)
Cl(1)	−0.3915(3)	0.4895(2)	−0.0757(1)
Cl(2)	−0.8372(4)	0.5814(2)	−0.0695(1)
Cl(3)	−0.7743(4)	0.4081(2)	−0.1425(1)

Table 2 Selected bond lengths (Å) and angles (°) in compound **I**

Fe(1)–C(1)	2.049(6)	Fe(1)–C(2)	2.058(6)
Fe(1)–C(3)	2.048(6)	Fe(1)–C(4)	2.051(6)
Fe(1)–C(5)	2.044(6)	Fe(1)–C(6)	2.054(6)
Fe(1)–C(7)	2.068(6)	Fe(1)–C(8)	2.060(6)
Fe(1)–C(9)	2.061(6)	Fe(1)–C(10)	2.048(6)
C(10)–C(19)	1.450(9)	C(19)–C(18)	1.337(9)
C(18)–C(17)	1.461(9)	C(17)–O(1)	1.232(7)
C(17)–C(16)	1.503(9)	C(12)–C(12)*	1.492(12)
C(9)–C(10)–C(19)	126.5(6)	C(6)–C(10)–C(19)	126.0(6)
C(10)–C(19)–C(18)	124.7(6)	C(19)–C(18)–C(17)	120.7(6)
C(18)–C(17)–C(16)	117.6(5)	C(18)–C(17)–O(1)	123.4(6)
C(16)–C(17)–O(1)	119.0(6)	N(11)–C(16)–C(17)	116.4(5)
C(15)–C(16)–C(17)	120.0(5)		

* Equivalent position relative to x, y, z: $-x-1, -y, -z$.

Suitable crystals were obtained by the slow diffusion of hexane into a solution of compound **I** in chloroform. They contain in the lattice two chloroform solvent molecules per molecule of **I**, which are slowly lost at room temperature. Accordingly, data were collected using low-temperature procedures. A view of the molecule **I** is presented in Fig. 1, and final atomic coordinates for non-hydrogen atoms and selected bond distances and angles are listed in Tables 1 and 2 respectively. The structure shows a 2,2′-bipyridine framework with the expected transoid conformation about the interannular C–C bond,[1,21] with the two 3-(ferrocenyl)-1-oxoprop-2-enyl groups covalently attached in the 6,6′ positions. The enone double bonds possess the *E* configuration predicted from the ^1H NMR spectrum of the compound. All bond lengths and angles within the molecule are as expected.

All in all, the structure is much as expected, and offers no clues as to the unreactivity in the ring-closure reaction. We merely note that we have observed a similar sluggishness in reactions of 2,6-di[3-(9-anthryl)-1-oxoprop-2-enyl]pyridine and 2,6-di[3-(1-naphthyl)-1-oxoprop-2-enyl]pyridine, suggesting a steric origin.[22] In view of these problems we have investigated route 2 for the synthesis of dfspy.

Table 3 Electrochemical data[a]

Compound	Ferrocene–ferrocenium	M^{II}–M^{III}	Reductions
I[b]	0.11		−1.60, −2.09
II[b]	0.17		−1.51, −1.93
bfterpy[b]	0.13		−1.46, −2.01
dfspy[b]	0.10		−1.50, −2.02
$[Fe(bfterpy)_2][PF_6]_2$	0.24	0.93	−1.17, −1.65
$[Co(bfterpy)_2][PF_6]_2$	0.29	0.57	−1.01, −1.42
$[Ni(bfterpy)_2][PF_6]_2$	0.25		−1.40, −1.66, −1.97
$[Zn(bfterpy)_2][PF_6]_2$	0.27		−1.49, −1.67, −1.84
$[Fe_2(dfspy)_2][PF_6]_4$	0.26	1.03	−0.63, −0.93, −1.09
$[Co_2(dfspy)_2][PF_6]_4$	0.26		−0.98, −1.14, −1.96, −2.07
$[Ni_2(dfspy)_2][PF_6]_4$	0.27		−1.25, −1.61, −1.87
$[Zn_2(dfspy)_2][PF_6]_4$	0.26		−1.41, −1.55, −1.74, −1.86

[a] Obtained using 0.1 mol dm^{-3} $[NBu_4][BF_4]$ as supporting electrolyte. Potentials in V and *vs.* ferrocene. Scan rate 0.1 V s^{-1}. Solvent MeCN unless otherwise stated. [b] In CH_2Cl_2.

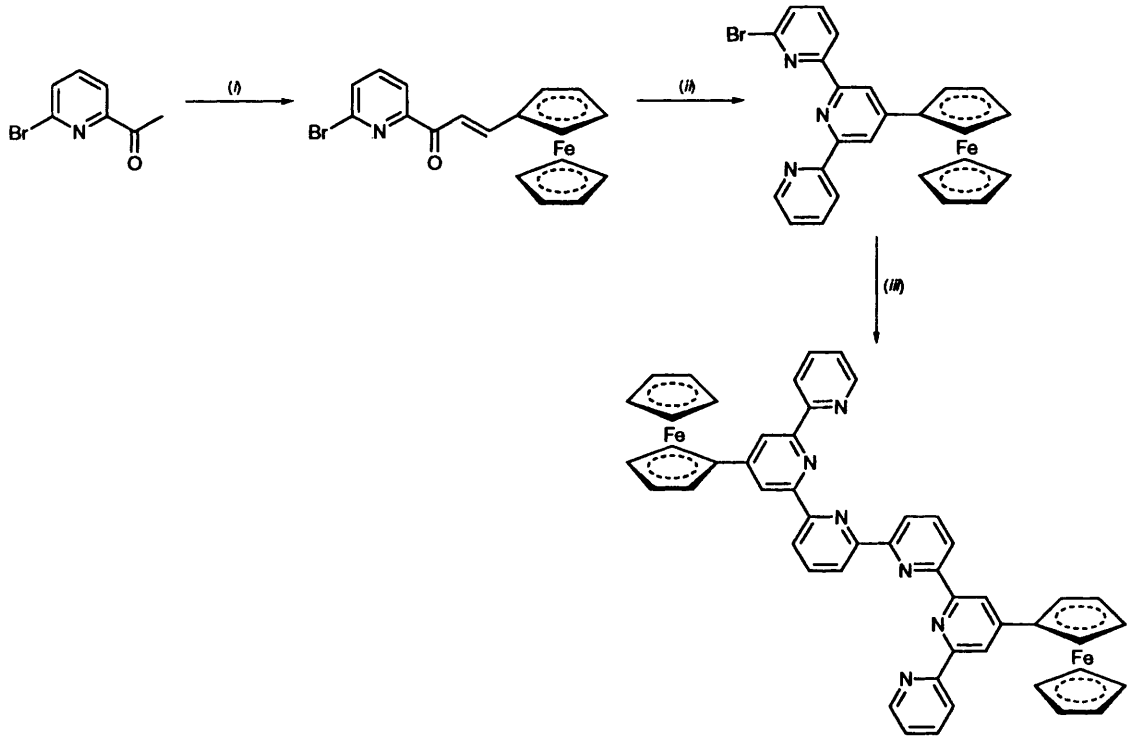

Scheme 2 (*i*) Ferrocenecarbaldehyde; (*ii*) [2-oxo-2-(2-pyridyl)ethyl]pyridinium iodide; (*iii*) $[Ni(H_2O)_6]Cl_2$, Zn, PPh_3, dimethylformamide

The reaction of 6,6′-di(1-pyridinioacetyl)-2,2′-bipyridine diiodide and 2-[3-(ferrocenyl)-1-oxoprop-2-enyl]pyridine in ethanol in the presence of ammonium acetate for 16 h gave a black solid (see Scheme 1, route 2). This crude product was recrystallized from toluene to yield dfspy as an orange solid in 20% yield. The FAB mass spectrum of this orange solid shows a parent ion at *m/z* 833, as expected for dfspy, and partial elemental analysis and IR data are also in agreement with the formulation as dfspy. The ^1H NMR spectrum of a solution of dfspy in $CDCl_3$ shows three signals for the ferrocenyl groups; a singlet at δ 4.15 for the C_5H_5 ring and two pseudo-triplets for the C_5H_4 protons of the substituted ring at δ 4.51 and 5.04. The ligand is symmetrical on the NMR time-scale and a total of nine signals are observed in the aromatic region and assigned to the protons from the pyridyl groups. The resonances from H^5, H^4 and $H^{4''}$ were unambiguously assigned from correlation spectroscopy (COSY) experiments; those for $H^{3'}$ and $H^{5'}$ are of ambiguous assignment and H^3, $H^{5''}$, H^6 and $H^{3''}$ appear overlapped in the range δ 8.70–8.82.

The new compound, dfspy, is also electroactive (Table 3) and exhibits a reversible Fe^{II}–Fe^{III} process at +0.10 V *versus* ferrocene with an i_a/i_c ratio equal to unity in dichloromethane solution. The data obtained are in close agreement with those reported for other ferrocene-functionalized oligopyridines.[3–12] The ΔE_p value found from cyclic voltammetry experiments and the half-peak width from differential pulse voltammetry are close to those found for the Fe^{II}–Fe^{III} process in ferrocene itself, suggesting that there is no interaction between the two redox-active centres in dfspy. Accordingly, the +0.10 V process represents two one-electron steps occurring at the same potential, similar to the behaviour observed for **I**.

Although we had succeeded in preparing dfspy, the relatively low yield (≈20%) and the large number of steps involved led us to consider one further approach (Scheme 2). This involved the symmetrical coupling of two 4′-ferrocenyl-substituted 6-halogeno-2,2′:6′,2″-terpyridines, a method which has been successfully used in the synthesis of spy[23] and its 4′,4‴-diaryl derivatives.[20] As a general procedure the route involves coupling of the appropriate 6-bromo-4′-X-2,2′:6′,2″-terpyridine to yield a double-helical nickel(II) complex $[Ni_2(4',4'''$-

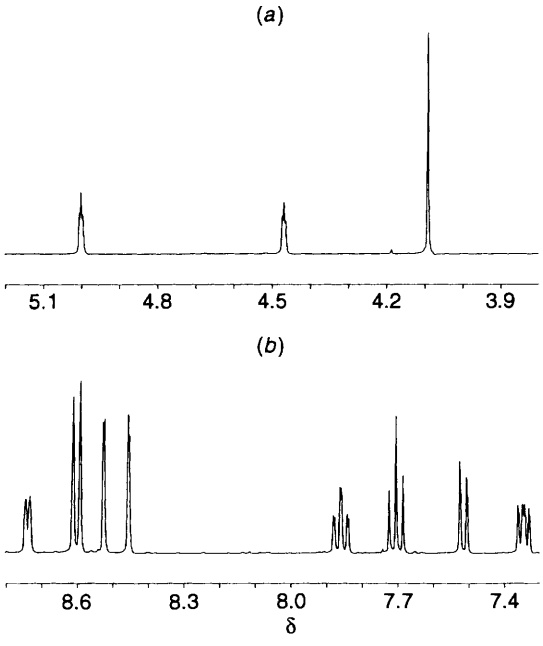

Fig. 2 Proton NMR spectrum of bfterpy (250 MHz, $CDCl_3$): (*a*) ferrocenyl protons and (*b*) pyridine protons

$X_2spy)_2]^{4+}$, from which the free ligand may be isolated in reasonable yield after demetallation with cyanide.

In order to explore the viability of the route with ferrocenyl substituents we have prepared the compound 6-bromo-4′-ferrocenyl-2,2′:6′,2″-terpyridine (bfterpy) using a Krohnke-type pyridine synthesis.[13] In the first step the enone 6-bromo-2-[3-(ferrocenyl)-1-oxoprop-2-enyl]pyridine **II** was obtained from the reaction of 2-acetyl-6-bromopyridine and ferrocenecarbaldehyde in the presence of aqueous sodium hydroxide. The enone exhibits a characteristic ν(C=O) stretching mode in its IR spectrum at 1661 cm^{-1}, and the formulation was confirmed by FAB mass spectroscopy (*m*/*z* = 395/397) and elemental analysis. The ^1H NMR spectrum shows three signals (one singlet and two pseudo-triplets) in the range δ 4.18–4.68, assigned to the ferrocenyl protons, and a total of five signals between δ 7.00 and 9.00 with an AB pattern at δ 7.72 and 7.90 assigned to the vinyl group and resonances at δ 7.64, 7.71 and 8.13 assigned to H^5, H^4 and H^3 respectively.

The reaction of compound **II** with *N*-[2-oxo-2-(2-pyridyl)ethyl]pyridinium iodide in ethanol in the presence of an excess of ammonium acetate resulted in the precipitation of bfterpy as an orange solid in good yield. The FAB mass spectrum exhibits an intense parent ion peak at *m*/*z* 495/497 and no absorptions assigned to carbonyl groups are observed in the IR spectrum. The ^1H NMR spectrum of $CDCl_3$ solutions of bfterpy (Fig. 2) exhibits three resonances assigned to the ferrocenyl groups and a total of nine for the terpyridyl protons. All resonances were assigned by COSY experiments except those for the $H^{3'}$ and $H^{5'}$ protons, for which the assignment remains ambiguous.

The electrochemical behaviour of compound **II** and bfterpy has been studied by cyclic voltammetry (Table 3); each compound shows a single reversible Fe^{II}–Fe^{III} process at anodic potentials (+0.17 and +0.13 V respectively). Each compound also exhibits two ill defined reduction waves.

Numerous attempts have been made to dimerize bfterpy using our standard conditions[23,24] {$[Ni(PPh_3)_n]$ (*n* = 3 or 4) prepared *in situ* from the reaction of $[Ni(H_2O)_6]Cl_2$ and Zn in dimethylformamide (dmf) in the presence of an excess of PPh_3}. After removal of the dmf *in vacuo*, water was added to give a deep purple solution. This was treated directly with potassium cyanide and heated to reflux for 1 h to give a brown precipitate. Recrystallization from dichloromethane–hexane gave an orange powder of variable and unreproducible composition. Proton NMR spectroscopic and FAB mass spectrometric studies on the various solids obtained showed the presence of the desired dfspy, together with variable amounts of bfterpy and 4′-ferrocenyl-2,2′:6′,2″-terpyridine (fterpy).

The compounds dfspy and bfterpy represent two new ferrocene-functionalized oligopyridines and their interactions with metal ions has been studied. The reaction of bfterpy with iron(II) chloride at room temperature gives blue solutions from which the deep blue complex $[Fe(bfterpy)_2][PF_6]_2$ can be obtained after the addition of $[NH_4][PF_6]$. The FAB mass spectrum of this salt exhibits ions corresponding to $[Fe(bfterpy)_2][PF_6]_2$, $[Fe(bfterpy)_2][PF_6]$ and $[Fe(bfterpy)_2]$, whilst the ^1H NMR spectrum is broadened and the resonances corresponding to the protons on the pyridine rings are shifted downfield. This is characteristic of a paramagnetic species and indicates that, in solution, the complex contains a high-spin iron(II) centre, in contrast to $[Fe(fterpy)_2][PF_6]_2$ which is diamagnetic.[8] We have not made detailed studies of the magnetic properties of this complex, but note that the complex $[Fe(bterpy)_2][PF_6]_2$ is also high spin.[20] Resonances at δ 3.2, 3.7 and 4.1 are assigned to the ferrocenyl groups [which are remote from the central, paramagnetic, iron(II) site]. The complex exhibits Fe^{II}–Fe^{III} processes at +0.24 and +0.93 V *vs.* ferrocene in its cyclic voltammogram (Table 3). The first is reversible and assigned to simultaneous redox reactions at the two pendant ferrocenyl groups, whilst that at +0.93 V is less well defined, only partially reversible ($i_a/i_p < 1$) and assigned to the central iron atom. The +0.24 V process becomes irreversible after passage through +0.93 V, suggesting an electrochemical–chemical–electrochemical process following oxidation of the central iron atom. The Fe^{II}–Fe^{III} process for the central metal atom is shifted to more positive potentials than observed for the complexes $[Fe(terpy)_2]^{2+}$ (+0.74 V), $[Fe(bterpy)_2]^{2+}$ (bterpy = 6-bromo-2,2′:6,6″-terpyridine) (+0.85 V) or $[Fe(fterpy)_2]^{2+}$ (+0.81 V). At cathodic potentials two poorly defined reduction processes were observed.

In a similar way, bfterpy reacts with $Co(O_2CMe)_2{\cdot}4H_2O$ to give the red complex $[Co(bfterpy)_2][PF_6]_2$. The FAB mass spectrum exhibits intense peaks corresponding to $[Co(bfterpy)_2][PF_6]_2$, $[Co(bfterpy)_2][PF_6]$ and $[Co(bfterpy)_2]$ and the ^1H NMR spectrum of a CD_3CN solution exhibits a total of 12 broad and paramagnetically shifted signals, in accord with a symmetrical six-co-ordinate solution species. The complex is redox-active, and processes were observed at +0.29 and +0.57 V *vs.* ferrocene, with the first peak being twice the intensity of the second (Table 3). The first process corresponds to the Fe^{II}–Fe^{III} redox couple and the second to the Co^{II}–Co^{III} couple. This latter process is fully reversible, and, in contrast to the behaviour of the iron(II) complex, the reversibility of the ferrocene-centred processes is not altered after passage through +0.57 V. The Co^{II}–Co^{III} process has been shifted to more positive potentials than for the complexes $[Co(fterpy)_2]^{2+}$ (−0.18 V) and $[Co(bterpy)_2]^{2+}$ (+0.47 V).

The reaction of $Ni(O_2CMe)_2{\cdot}4H_2O$ with bfterpy, followed by the addition of ammonium hexafluorophosphate, yields the complex $[Ni(bfterpy)_2][PF_6]_2$ as a red solid the FAB mass spectrum of which exhibits peaks for $[Ni(bfterpy)_2][PF_6]_2$, $[Ni(bfterpy)_2][PF_6]$ and $[Ni(bfterpy)_2]$. The ^1H NMR spectrum exhibits broad and paramagnetically shifted peaks, but resonances at δ 4.9, 5.2 and 7.4 may be assigned to the ferrocenyl protons. The cyclic voltammogram in acetonitrile solution exhibits a single reversible process at +0.25 V *vs.* ferrocene assigned to the simultaneous oxidation of the two ferrocenyl groups (Table 3). No peaks were found at higher potentials indicating that the nickel(III) state is not accessible. A number of reduction processes were observed at negative potentials

Finally, the zinc complex $[Zn(bfterpy)_2][PF_6]_2$ was

prepared by the reaction of solutions of bfterpy and zinc acetate. The FAB mass spectrum shows peaks corresponding to the fragments $[Zn(bfterpy)_2][PF_6]_2$, $[Zn(bfterpy)_2][PF_6]$ and $[Zn(bfterpy)_2]$, whilst the ^1H NMR spectrum shows three signals for the ferrocenyl groups and a total of nine signals for the pyridine protons, indicating that the bfterpy ligands are equivalent in the complex. All resonances were assigned by COSY experiments. The compound exhibits a single reversible Fe^{II}–Fe^{III} process at +0.27 V *vs.* ferrocene for the ferrocenyl groups as well as several poorly defined reduction processes (Table 3).

We have carried out differential pulse-voltammetry experiments on all of these complexes, and in each case the half-peak width found for Fe^{II}–Fe^{III} process of ferrocenyl groups is close to that for ferrocene, providing further support for our contention that there is little interaction between the pendant groups.[25,26]

Table 4 Visible absorption spectra

Compound	$\lambda_{max}(\varepsilon)$*
I	521 (5960)
II	531 (3655)
bfterpy	365 (2280), 461 (1050)
dfspy	446 (4270), 349 (6340)
$[Fe(bfterpy)_2][PF_6]_2$	570 (9060)
$[Co(bfterpy)_2][PF_6]_2$	545 (6370)
$[Ni(bfterpy)_2][PF_6]_2$	409 (3400), 536 (6530)
$[Zn(bfterpy)_2][PF_6]_2$	410 (3340), 538 (6520)
$[Fe_2(dfspy)_2][PF_6]_4$	571 (13 820)
$[Co_2(dfspy)_2][PF_6]_4$	556 (11 900)
$[Ni_2(dfspy)_2][PF_6]_4$	546 (11 900)
$[Zn_2(dfspy)_2][PF_6]_4$	410 (6611), 555 (11 900)

* λ in nm, ε in $dm^3\ mol^{-1}\ cm^{-1}$.

The colours of the new compound and its complexes are of some interest. The principle chromophore is the pendant ferrocenyl group; accordingly, the zinc complex $[Zn(bfterpy)_2][PF_6]_2$ is a red solid, in contrast to colourless $[Zn(bterpy)_2][PF_6]_2$.[20] The compound bfterpy is orange-yellow and exhibits bands in its electronic spectrum at 365 and 461 nm with relatively low absorption coefficients. However, when bfterpy is co-ordinated to iron(II), cobalt(II), nickel(II) or zinc(II), intensely violet-red compounds are obtained. The visible region of the absorption spectra is characterized by a band at 540–570 nm with $\varepsilon \approx 6500\ dm^3\ mol^{-1}\ cm^{-1}$ for the cobalt(II), nickel(II) and zinc(II) complexes and of $\approx 9000\ dm^3\ mol^{-1}\ cm^{-1}$ for the iron(II) species (see Table 4). The nickel(II) and zinc(II) complexes also exhibit a well defined band at 410 nm, whilst this appears as a shoulder on an intense absorption for the iron(II) and cobalt(II) complexes.

The co-ordination behaviour of the ferrocene-functionalized sexipyridine, dfspy, has also been studied. The compound spy and its derivatives have been shown to co-ordinate to metal ions in a variety of ways, dictated by the favoured co-ordination numbers and geometries of the metal centres. Metal ions with high co-ordination numbers can co-ordinate all of the six nitrogen-donor atoms, as observed in the cation $[Eu(spy)(NO_3)_2]^+$.[27] The consequences of co-ordination to metal ions with lower co-ordination numbers are of more interest, and it has been shown that these ligands can be partitioned into a variable number of metal-binding domains to give double-helical complexes. For example, dinuclear double helicates $[M_2L_2]^{n+}$ are obtained as a result of partitioning of the ligands into two tridentate domains upon interaction with six-co-ordinate metal centres, whilst trinuclear double helicates $[M_3L_2]^{n+}$ are the consequence of the ligand presenting three didentate domains to four-co-ordinate metal ions (Fig. 3).[14,18,23] The presence of substituents does not appreciably alter this helication behaviour.

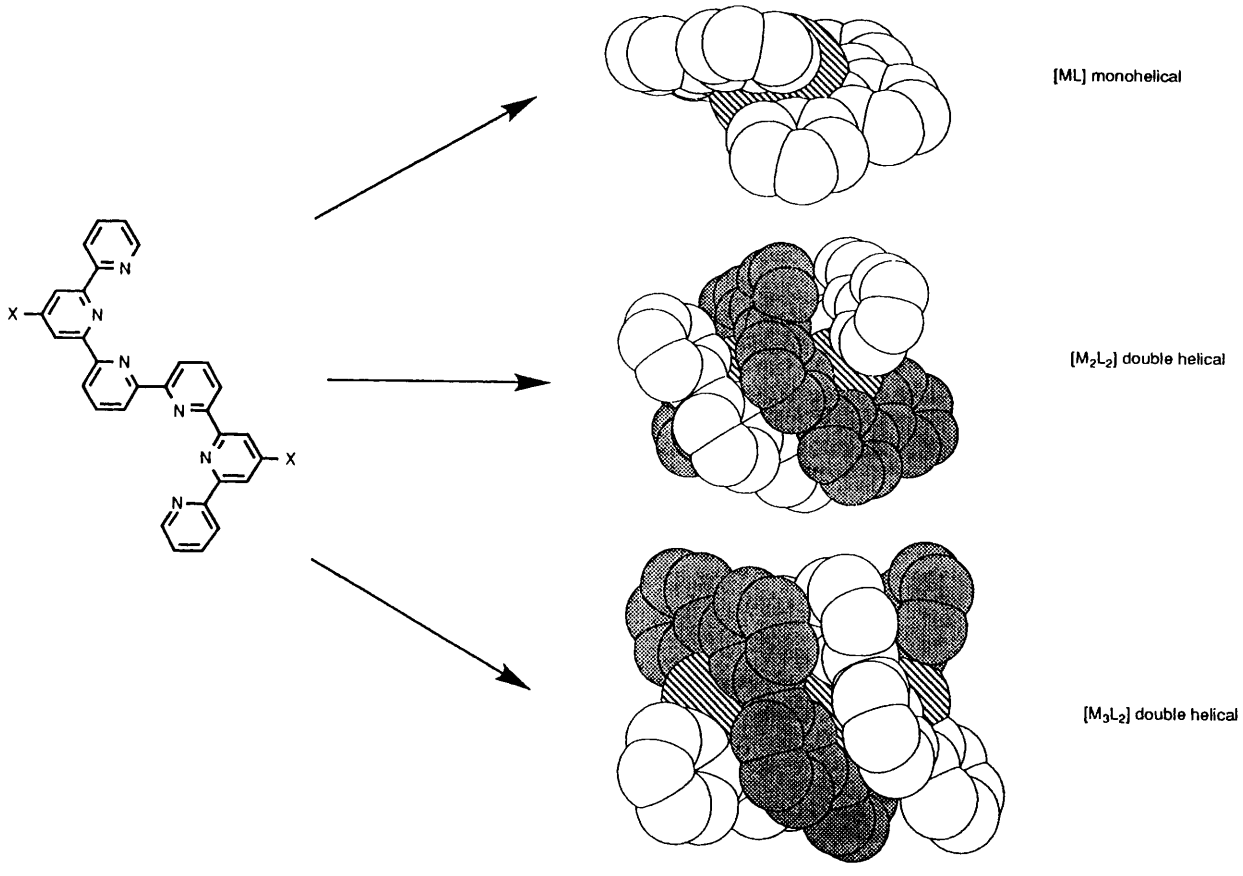

Fig. 3 The co-ordination behaviour of spy compounds

Although the compound dfspy is only slightly soluble in methanol, reaction with $FeCl_2 \cdot 4H_2O$ in boiling methanol gives dark coloured solutions. After a few minutes at reflux, thin-layer chromatography (TLC) shows the presence of a major reddish and a minor violet product. After 1 h the quantity of the reddish component has decreased whereas that of the violet one has increased; small amounts of other coloured products were also noted. The reaction mixture was evaporated to dryness after 1.5 h and chromatographed (eluent, 30:2:1 MeCN, aqueous saturated KNO_3 solution, water). The red and violet fractions were collected separately, and addition of aqueous $[NH_4][PF_6]$ resulted in the precipitation of red and violet solids respectively. The violet solid was the major product from the reaction, and elemental analysis gives a stoichiometry $Fe(dfspy)(PF_6)_2$, whilst the observation in the FAB mass spectrum of intense peaks corresponding to the fragments $[Fe_2(dfspy)_2][PF_6]_3$, $[Fe_2(dfspy)_2][PF_6]_2$ and [Fe(dfspy)] suggests that the compound should be formulated as the dinuclear double helicate $[Fe_2(dfspy)_2][PF_6]_4$. This is in accord with the expected formation of double-helical complexes in which the ligands are partitioned into two tridentate domains, with each metal ion in an N_6 environment composed of a tridentate domain from each ligand.[14,18] In such a conformation the ligands are symmetrical about the central interannular C–C bond (between rings C and D). The ^1H NMR spectrum shows a total of 13 broad and paramagnetically shifted signals, of which nine are assigned to the pyridine-ring protons of the dfspy ligands, in accord with the symmetry.

The complex is electrochemically active and an acetonitrile solution of the complex shows Fe^{II}–Fe^{III} processes at +0.26 and +1.03 V *vs.* ferrocene. The first (reversible) process is assigned to the ferrocene groups and becomes irreversible after passage through the +1.03 V process. The latter is assigned to the oxidation of the six-co-ordinate iron centres and is broad and irreversible. This behaviour is in contrast with that of the complex $[Fe_2(spy)_2][PF_6]_4$ (spy = 2,2′:6′,2″:6″,2‴:6‴,2⁗:6⁗,2⁗′-sexipyridine)[14] which exhibits two reversible Fe^{II}–Fe^{III} processes at +0.96 and +1.11 V. The irreversibility with the complex of dfspy is presumably related to the high charge build-up resulting from the formation of the $[Fe_2(dfspy)_2]^{8+}$ cation after the first redox process. Further oxidation processes at the central six-co-ordinate metal ions can occur (involving the formation of species with charge +9 and +10) but these are followed by degradative chemical processes. The complex also shows three poorly resolved ligand-based reductions at −0.63, −0.93 and −1.09 V.

In a similar manner, dfspy dissolves upon heating with methanolic $Co(O_2CMe)_2 \cdot 4H_2O$ to give coloured solutions; after several minutes TLC shows the presence of a reddish and a violet species. After 1.5 h at reflux the violet compound predominates, although some other minor products are also present. The violet fraction was collected after column chromatography on silica MeCN–aqueous saturated KNO_3 solution–water (30:2:1) and addition of $[NH_4][PF_6]$ resulted in the deposition of a solid. Elemental analysis suggested a stoichiometry $Co(dfspy)(PF_6)_2$, whilst the FAB mass spectrum exhibited peaks for $[Co_2(dfspy)_2][PF_6]_3$, $[Co_2(dfspy)_2][PF_6]_2$, $[Co_2(dfspy)_2][PF_6]$ and [Co(dfspy)]. Once again, a dinuclear double-helical formulation for the complex is appropriate, $[Co_2(dfspy)_2][PF_6]_4$. As expected, the complex is paramagnetic, and the ^1H NMR spectrum of a CD_3CN solution shows a total of 13 broad and paramagnetically shifted resonances in the range δ −40.5 to 154.4. The cyclic voltammogram of acetonitrile solutions of this complex shows only a reversible oxidation process at +0.26 V *vs.* ferrocene attributed to oxidation of the four ferrocene groups. No other oxidation processes were observed, in contrast to the complex $[Co_2(spy)_2][PF_6]_4$, for which two reversible processes assigned to the couples $Co^{II}Co^{II}$–$Co^{III}Co^{II}$ and $Co^{III}Co^{II}$–$Co^{III}Co^{III}$ occur at +0.44 and +0.77 V, respectively.[14] Although this difference in behaviour must be related to the presence of positively charged ligands after the oxidation of the ferrocenyl groups, it is difficult fully to rationalize. The complex also exhibits four reduction waves centred at −0.98, −1.14, −1.96 and −2.07 V; the first three are reversible whereas the fourth shows a ΔE_p of 110 mV.

Nickel(II) complexes are readily prepared from the reaction of dfspy with nickel acetate in boiling methanol. Thin-layer chromatography of the reaction mixture after 1.5 h shows the presence of two (reddish and violet) compounds, which can be separated by column chromatography on silica. The compounds were isolated as their hexafluorophosphate salts, and the FAB mass spectrum of the violet compound showed peaks for $[Ni_2(dfspy)_2][PF_6]_3$, $[Ni_2(dfspy)_2][PF_6]_2$ and [Ni(dfspy)], respectively. These data suggest that the complex should be formulated as double-helical $[Ni_2(dfspy)_2][PF_6]_4$. A total of 12 broad and paramagnetically shifted signals were observed in the ^1H NMR spectrum. The complex is electroactive, and the cyclic voltammogram of an acetonitrile solution shows a reversible process at +0.27 V *vs.* ferrocene assigned to the oxidation of the four ferrocenyl groups. No other oxidation processes were observed, but three poorly resolved reduction processes were found at −1.25, −1.61 and −1.87 V.

The reaction of dfspy with zinc(II) acetate in refluxing methanol results in the formation of deep coloured solutions. Thin-layer chromatography of these solutions after several minutes and after 1.5 h showed no appreciable differences, and a major violet fraction was separated by column chromatography and the hexafluorophosphate salt precipitated by the addition of $[NH_4][PF_6]$. The FAB mass spectroscopy of this salt exhibits peaks assigned to $[Zn_2(dfspy)_2][PF_6]_3$, $[Zn_2(dfspy)_2][PF_6]_2$ and [Zn(dfspy)] suggesting a double-helical conformation of the dfspy ligands around two six-co-ordinate zinc(II) centres. The complex should then be formulated as $[Zn_2(dfspy)_2][PF_6]_4$. This complex is obtained as a red solid in contrast to the colourless compound $[Zn_2(spy)_2][PF_6]_4$.[14] The electronic spectra of the cobalt(II), nickel(II) and zinc complexes each show in the visible region a band centred at 545–555 nm with ε values of about 12 000 $dm^3\ mol^{-1}\ cm^{-1}$. The iron complex shows a shift of this band to a higher wavelength and shows also a larger ε value. The zinc complex also shows a well defined band at 410 nm which is present as a shoulder for the remaining complexes.

The ^1H NMR spectrum of the (diamagnetic) zinc complex is of considerable interest as it may be fully assigned (Fig. 4). A total of five signals are observed for the ferrocene groups. The resonance at δ 4.31 represents 20 protons and is assigned to the C_5H_5 ferrocenyl rings, whereas four signals at δ 4.95, 4.98, 5.43 and 5.48, each integrating to four protons, are assigned to the C_5H_4 rings. This suggests that constraints in the free rotation around the C_5H_4–terpy bond results in the observation of α, α′, β′ and β protons as a result of the two sides of the C_5H_4 ring being in different environments. We can eliminate the possibility of the two different ferrocene groups in each ligand being in different environments from the high symmetry observed for the oligopyridine (nine resonances). This restricted rotation is presumably the reason why four ferrocene resonances are observed in the ^1H NMR spectra of the iron(II) and cobalt(II) complexes, although paramagnetic broadening prevents further investigation in these cases. Unambiguous assignments were made by two-dimensional (COSY) studies, with the exception of the H^3, $H^{3'}$, $H^{5'}$, $H^{3''''}$, $H^{3'''}$, $H^{5''''}$, $H^{3'''}$ and $H^{3''}$ protons which appear in the range δ 8.44–8.54 as an overlapping set of multiplets.

The zinc complex is electroactive and exhibits a reversible Fe^{II}–Fe^{III} process at +0.26 V assigned to the four ferrocene substituents and ligand-based reductions at −1.41, −1.55, −1.74 and −1.86 V.

The reddish compounds obtained from the reactions of dfspy with iron(II) and nickel(II) have not been fully characterized, but FAB mass spectrometric studies strongly suggest a mononuclear formulation. Thus, the iron(II) complex exhibits peaks at *m/z* 887, 1031, 1865 and 2010 assigned to the mononuclear species

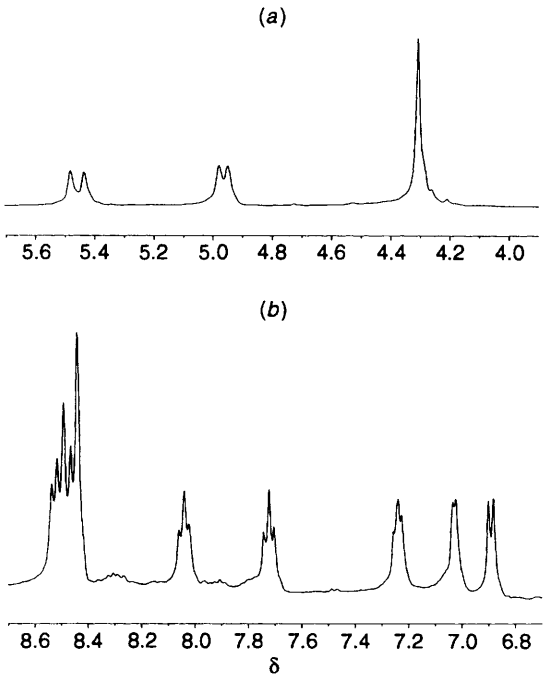

Fig. 4 Proton NMR spectrum of the double-helical complex $[Zn_2(dfspy)_2]^{4+}$ (250 MHz, $CDCl_3$): (*a*) ferrocenyl protons and (*b*) pyridine protons

[Fe(dfspy)], [Fe(dfspy)][PF_6], [Fe(dfspy)$_2$][PF_6] and [Fe(dfspy)$_2$][PF_6]$_2$, respectively. No significant amounts of mononuclear complexes were found from the reactions with cobalt(II) or zinc(II). This contrasts with the behaviour of spy itself which seems to give only dinuclear double-helical complexes with these metal ions.[14]

In conclusion, we have shown that the helication behaviour of 2,2′:6′,2″:6″,2‴:6‴,2⁗:6⁗,2⁗′-sexipyridines is not altered upon the introduction of substituents. The reversibility of redox processes associated with metal ions co-ordinated to the terpy domains of the ligand dfspy is affected if they occur after ferrocene-centred Fe^{II}–Fe^{III} processes have occurred. The new compound bfterpy has also been investigated and shown to have a rich co-ordination chemistry.

Acknowledgements

We thank the SERC, the European Community, the Schweizerischer Nationalfonds zur Förderung der wissenschaftlichen Forschung, the Comisión Interministerial de Ciencia y Technologia (PB91-0807-C02) and the Ministerio de Educación y Ciencia for support.

References

1 E. C. Constable, *Tetrahedron*, 1992, **48**, 10013; *Chem. Ind.* (*London*), 1994, 56; *Prog. Inorg. Chem.*, 1994, **42**, 67 and refs. therein.
2 D. Armspach, E. C. Constable, C. E. Housecroft, M. Neuburger, and M. Zehnder, *Supramol. Chem.*, in the press.
3 A. Benito, J. Cano, R. Martínez-Máñez, J. Soto, J. Payá, F. Lloret, M. Julve, J. Faus and M. D. Marcos, *Inorg. Chem.*, 1993, **32**, 1197; A. Benito, J. Cano, R. Martínez-Máñez, J. Soto, M. J. L. Tendero, J. Payá and E. Sinn, *Inorg. Chim. Acta*, 1993, **210**, 233; A. Benito, J. Cano, R. Martínez-Máñez, J. Payá, J. Soto, M. Julve, F. Lloret, M. D. Marcos and E. Sinn, *J. Chem. Soc., Dalton Trans.*, 1993, 1999.
4 I. R. Butler and J.-L. Roustan, *Can. J. Chem.*, 1990, **68**, 2212; I. R. Butler, *Organometallics*, 1992, **11**, 74; *Polyhedron*, 1992, **11**, 3117; I. R. Butler, N. Burke, L. J. Hobson and H. Findenegg, *Polyhedron*, 1992, **11**, 2435; I. R. Butler, M. Kalaji, L. Nehrlich, M. Hursthouse, A. I. Karaulov and K. M. Abdul Malik, *J. Chem. Soc., Chem. Commun.*, 1995, 459.
5 C. Chambron, C. Coudret and J.-P. Sauvage, *New J. Chem.*, 1992, **16**, 361.
6 P. D. Beer, O. Kocian, R. J. Mortimer and P. Spencer, *J. Chem. Soc., Chem. Commun.*, 1992, 602; P. D. Beer, O. Kocian and R. J. Mortimer, *J. Chem. Soc., Dalton Trans.*, 1990, 3283; P. D. Beer and H. Sikanyika, *Polyhedron*, 1990, **9**, 1091; P. D. Beer, *Chem. Soc. Rev.*, 1989, **18**, 409; P. D. Beer, E. L. Tite and A. Ibbotson, *J. Chem. Soc., Dalton Trans.*, 1991, 1691; C. D. Hall, J. H. R. Tucker and N. W. Sharpe, *Organometallics*, 1991, **10**, 1727; T. Saji and I. Kinoshita, *J. Chem. Soc., Chem. Commun.*, 1986, 716; E. W. Neuse, M. G. Meirim and N. F. Blum, *Organometallics*, 1988, **7**, 2562; D. Astruc, J. R. Hamon, G. Althoff, E. Román, P. Batail, P. Michaud, J. P. Mariot, F. Varret and D. Cozak, *J. Am. Chem. Soc.*, 1979, **101**, 5445.
7 B. Farlow, T. A. Nile, J. L. Walsh and A. T. McPhail, *Polyhedron*, 1993, **12**, 2891.
8 E. C. Constable, A. J. Edwards, R. Martínez-Máñez, P. R. Raithby and A. M. W. Cargill Thompson, *J. Chem. Soc., Dalton Trans.*, 1994, 645.
9 E. C. Constable, R. Martínez-Máñez, A. M. W. Cargill Thompson and J. V. Walker, *J. Chem. Soc., Dalton Trans.*, 1994, 1585.
10 E. C. Constable, A. J. Edwards, M. D. Marcos, R. Martínez-Máñez, P. R. Raithby and M. J. L. Tendero, *Inorg. Chim. Acta*, 1994, **224**, 11.
11 I. R. Butler, S. J. McDonald, M. B. Hursthouse and K. M. Abdul Malik, *Polyhedron*, 1995, **14**, 529.
12 E. C. Constable, A. J. Edwards, P. R. Raithby, J. Soto, M. J. L. Tendero and R. Martínez-Máñez, *Polyhedron*, in the press.
13 F. Krohnke, *Synthesis*, 1976, 1.
14 E. C. Constable, M. D. Ward and D. A. Tocher, *J. Chem. Soc., Dalton Trans.*, 1991, 1675; *J. Am. Chem. Soc.*, 1990, **112**, 1256.
15 J. E. Parks, B. E. Wagner and R. H. Holm, *J. Organomet. Chem.*, 1973, **56**, 53.
16 SHELXTL PLUS, Program version 4.0, Siemens Analytical X-Ray Instruments, Madison, WI, 1990.
17 G. M. Sheldrick, SHELXL 93, University of Göttingen, 1993.
18 K. T. Potts, M. Keshavarz-K, F. S. Tham, H. D. Abruna and C. Arana, *Inorg. Chem.*, 1993, **32**, 4436; K. T. Potts, K. A. Gheyson Raiford and M. Keshavarz-K, *J. Am. Chem. Soc.*, 1993, **115**, 2793; K. T. Potts, M. Keshavarz-K, F. S. Tham, H. D. Abruna and C. Arana, *Inorg. Chem.*, 1993, **32**, 4450.
19 E. C. Constable, P. Harverson, D. R. Smith and L. A. Whall, *Tetrahedron*, 1994, **50**, 7799.
20 R. Chotalia, Ph.D. Thesis, Cambridge, 1993.
21 E. C. Constable, *Adv. Inorg. Chem. Radiochem.*, 1987, **30**, 69.
22 E. C. Constable and D. Smith, unpublished work.
23 E. C. Constable and R. Chotalia, *J. Chem. Soc., Chem. Commun.*, 1992, 64.
24 E. C. Constable and M. D. Ward, *J. Chem. Soc., Dalton Trans.*, 1990, 1405; E. C. Constable, M. J. Hannon and D. A. Tocher, *Angew. Chem., Int. Ed. Engl.*, 1992, **104**, 218; *J. Chem. Soc., Dalton Trans.*, 1993, 1883; E. C. Constable, M. J. Hannon, A. J. Edwards and P. R. Raithby, *J. Chem. Soc., Dalton Trans.*, 1994, 2669; E. C. Constable, S. M. Elder, J. A. Healy and D. A. Tocher, *J. Chem. Soc., Dalton Trans.*, 1990, 1669.
25 J. B. Flanagan, S. Margei, A. J. Bard and F. C. Anson, *J. Am. Chem. Soc.*, 1978, **100**, 4.
26 D. E. Richardson and H. Taube, *Inorg. Chem.*, 1981, **20**, 1278.
27 E. C. Constable, R. Chotalia and D. A. Tocher, *J. Chem. Soc., Chem. Commun.*, 1992, 771.

Received 3*rd April* 1995; *Paper* 5/02103K